Supplementary Information

Reverse Flow Enhanced Inertia Pinched Flow Fractionation

Saijie Wang[1], Quanchen Xu[1], Zhihan Zhang[1], Shengbo Chen[1], Yizhou Jiang[1, 2], Zhuowei Feng[1], Dou Wang[1, *], Xingyu Jiang[1, *]

1 Shenzhen Key Laboratory of Smart Healthcare Engineering, Guangdong Provincial Key Laboratory of Advanced Biomaterials, Department of Biomedical Engineering, Southern University of Science and Technology, No. 1088 Xueyuan Rd, Nanshan District, Shenzhen. Guangdong 518055, China.

2 State Key Laboratory of Cardiovascular Disease, Fuwai Hospital, National Center for Cardiovascular Diseases, Chinese Academy of Medical Sciences and Peking Union Medical College, Beijing 100037, China.

* Corresponding author's email: wangd9@sustech.edu.cn (Dou Wang), jiang@sustech.edu.cn (Xingyu Jiang)

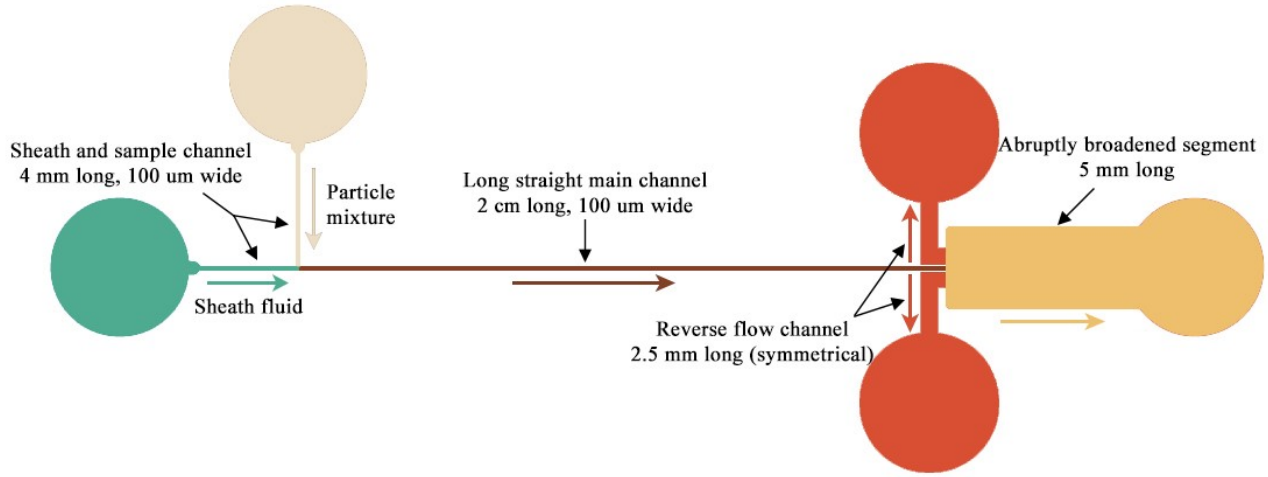

Figure S1. Structure of the RF-iPFF devices. RF-iPFF can be divided into five parts: the sheath fluid channel with inlet (Light Green), the particle channel with inlet (Light Brown), the long straight main channel (Dark Brown), the symmetrically distributed reverse flow channels with outlets (Dark Orange), and the abruptly broadened segment with outlet (Brownish Yellow).

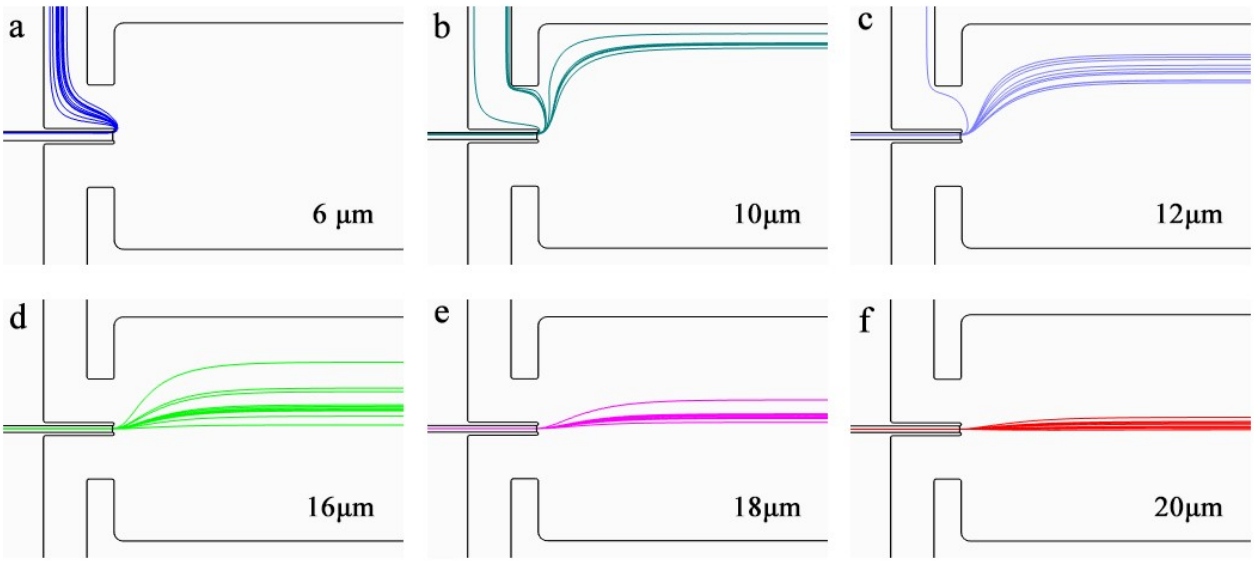

Figure S2. Simulated streamlines for particles of different sizes based on the RF-iPFF geometric model. (a - f) The flow rate is 2 mL/h, and the flow rate ratio is 10. The reverse flow opening size is 480 μm, accounting for 40 % of the half-width of the abruptly broadened segment. The width of the abruptly broadened segment is 2500 μm.

Although the particles released by each running program have the same particle size, the calculated results show that, for a specific particle size value, the streamline distribution still appears as a range rather than a specific line. This is because the release position of the particles is random. In the particle channel, there is also a velocity field in which the velocity in the center is fast and the velocity in the channel wall is slow. The varying release positions of the particles result in distinct initial conditions for each particle. In particular, the particles are involved in turning when they enter the long straight main channel from the particle channel. Thus, although the numerical results are convergent, they are also oscillating.

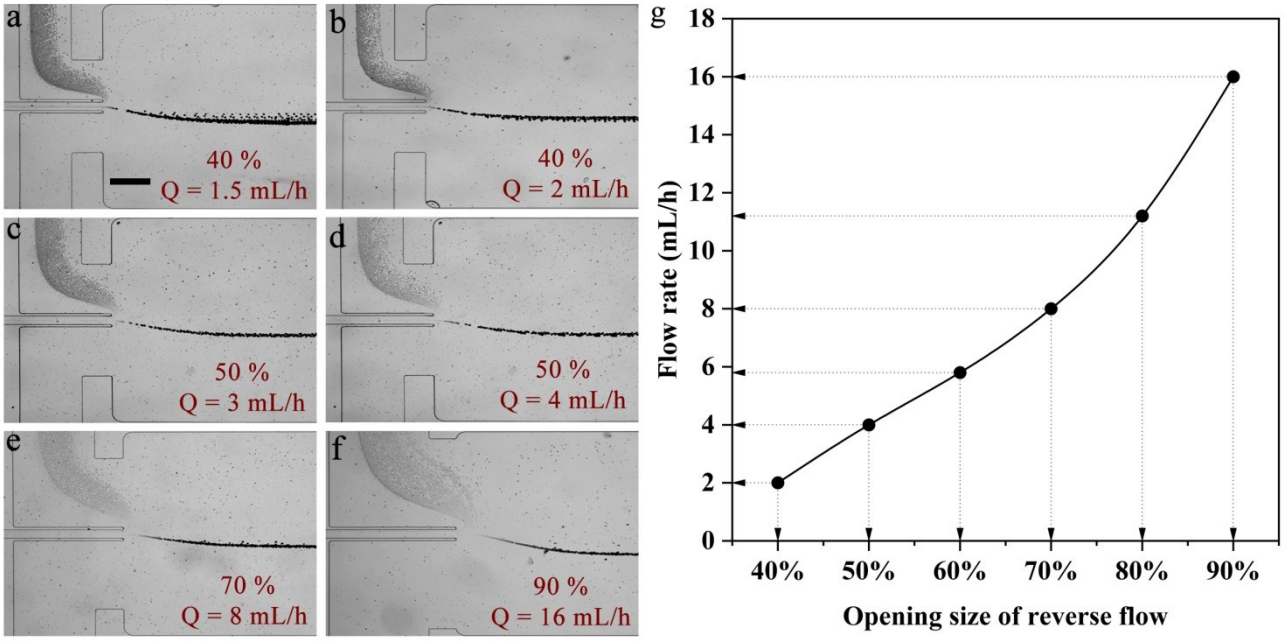

Figure S3: The minimum opening size required to carry nearly all 6 μm particles into the reverse flow channel at the marked flow rate. The flow rate ratio was controlled to be 10. (a-f) Superimposed images correspond to different flow rates. Note that the reverse flow opening size is not all the same, with other variables having the same parameters. The diameter of small particles is 6 μm, and the diameter of large particles is 20 μm. The scale bar represents 500 μm. (g) The relationship between different opening sizes and flow rates under the premise that all of the 6 μm particles can be carried into the reverse flow channel. The data corresponding to 60% and 80% of the abscissa are obtained by cubic spline interpolation.

The device is still functional at flow rates above 16 mL/h (Re = 59.3). Nearly all 6 μm particles can be carried into the reverse flow channel at Q = 16 mL/h (Figure S3f). If the flow rate continues to increase, there will be some 6 μm particles that cannot enter the reverse flow channel. This is because the influence of inertial force begins to increase while the influence of viscous force relatively weakens. Specifically, 6 μm particles are more obviously affected by inertia when they are deflected after entering the abruptly broadened segment, so they show a stronger tendency to move forward, and this tendency reduces the deflection angle of the particles. Nevertheless, particles of two different sizes can still be effectively separated.

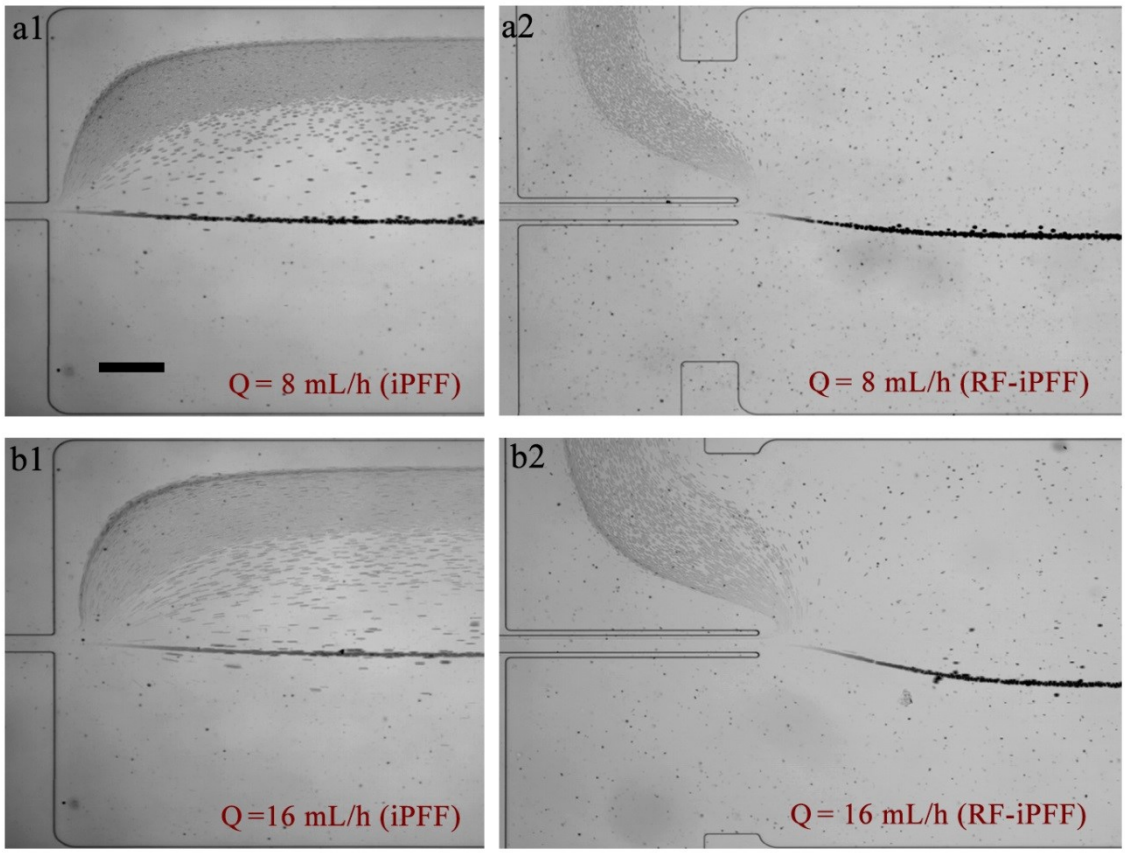

Figure S4: Comparison of RF-iPFF and traditional iPFF. (a1-a2) In comparing the separation effects of the two devices at 8 mL/h, other parameters such as flow rate ratio (α = 10) were consistent. (b1-b2) In comparing the separation effects of the two devices at 16 mL/h, other parameters such as flow rate ratio (α = 10) were consistent. The scale bar represents 400 um.

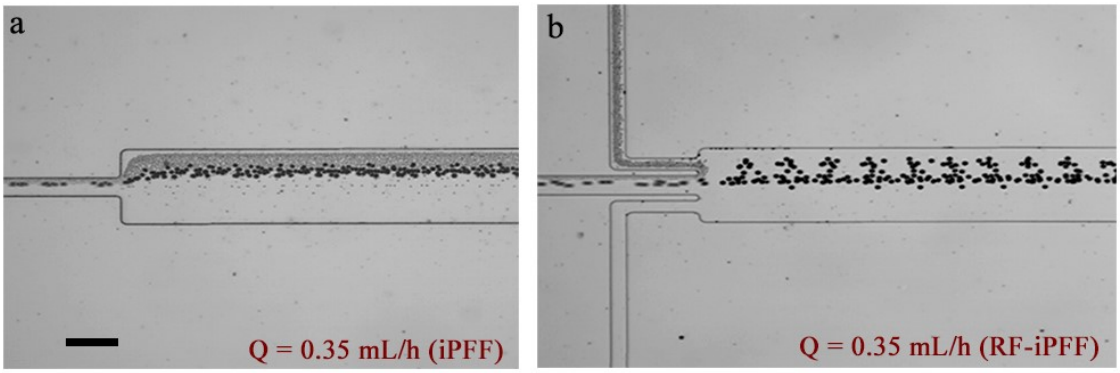

Figure S5: Comparison of separation performance between RF-iPFF and iPFF at low flow rates. Other parameters such as flow rate ratio (α = 10) were consistent. The scale bar represents 300 μm.

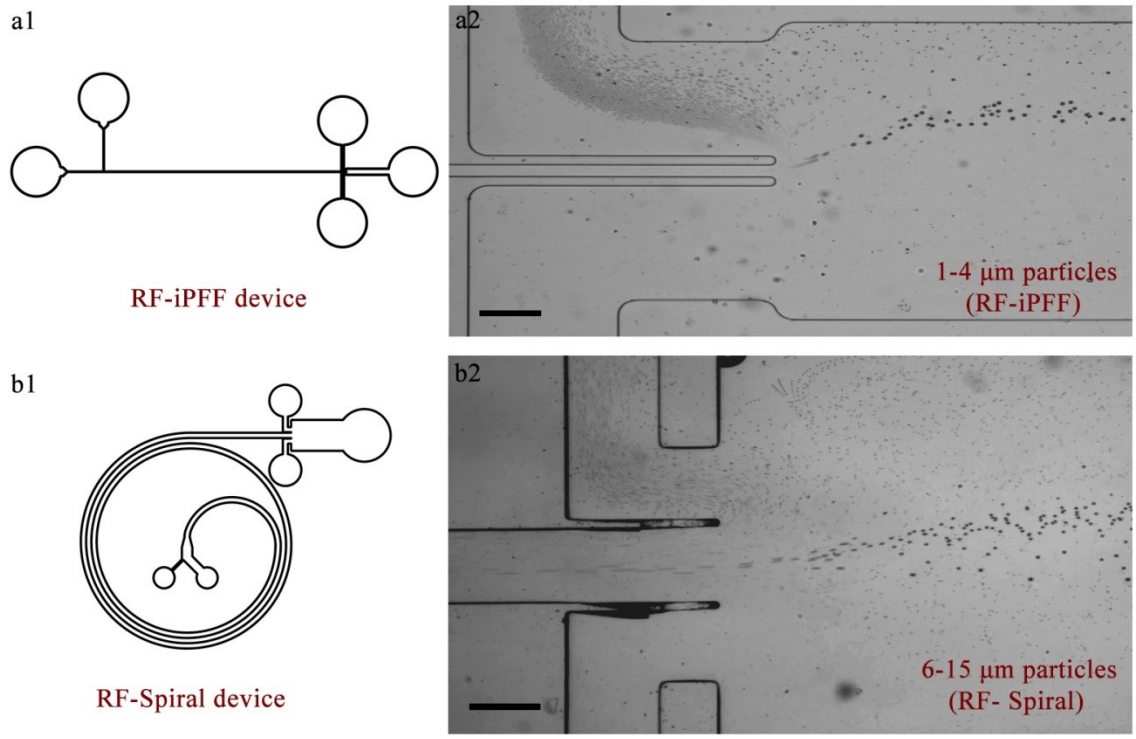

Figure S6: The applicability research of reverse flow enhancement effect. (a1) Schematic diagram of RF-iPFF device, the main parameters of the channel are determined based on the scaling law, designed to separate 1 μm and 4 μm particles. Drawings can be found in Supplementary Information. (a2) The separation effect of 1 μm and 4 μm particles based on RF-iPFF. (b1) Schematic diagram of RF-Spiral device, derived from modifying traditional spiral separation devices, designed to separate 6 μm and 15 μm particles. Drawings can be found in Supplementary Information. (b2) The separation effect of 6 μm and 15 μm particles based on RF-Spiral. The scale bar represents 100 μm applies to (a), and the scale bar represents 500 μm applies to (b).

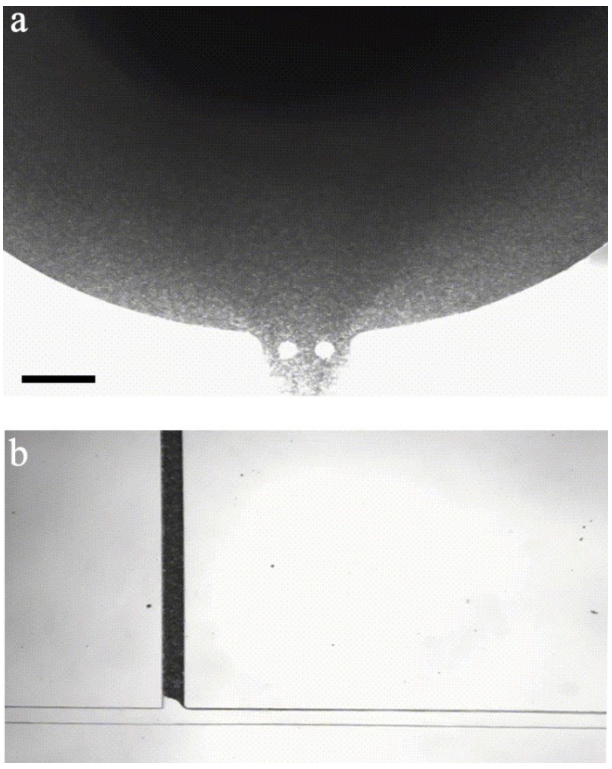

Figure S7: Images of untreated blood in the microfluidic device. The black dots are all blood cells, most of which are red blood cells. (a) Photograph of red blood cells at the entrance of the particle channel. (b) Photograph of red blood cells within the particle channel and upon entering the main channel, being focused by the sheath fluid towards the side wall of the main channel. The scale bar represents 400 μm.